ACI STRUCTURAL JOURNAL TECHNICAL PAPER

Title No. 118-S32

Cracking and Crushing in Prestressed Concrete Beams

by Federico Accornero, Renato Cafarelli, and Alberto Carpinteri

The cohesive/overlapping crack model represents an effective tool in the study of failure transition phenomena occurring in plain or reinforced concrete structures. In the present paper, this non-linear fracture mechanics model is applied to study the global structural behavior of prestressed concrete beams casted by means of pre-tensioning technique or, more generally, having a straight steel strand layout. In this context, a thorough analysis of scale effects is presented to investigate local mechanical instabilities such as snap-back and snap-through phenomena due to concrete cracking or crushing, highlighting the crucial role of the ductile-to-brittle transition in the design of prestressed concrete structural elements.

Keywords: concrete cracking; concrete crushing; ductile-to-brittle transition; non-linear fracture mechanics; prestressed concrete; scale effects.

INTRODUCTION

The flexural behavior of reinforced and prestressed concrete structural elements is affected by the presence of non-linear phenomena occurring during their loading processes, such as crack opening and advancement in tension, concrete crushing in compression, and steel yielding or slippage. In current design codes, these phenomena are not completely considered, due to the shortcomings present in the classical constitutive laws commonly adopted for materials. This framework may lead to unsafe structural behaviors due to stability losses that may occur during the loading process and involving snap-back or snap-through discontinuous phenomena. Furthermore, classical constitutive laws adopted for prestressed concrete structures are not able to capture the ductile-to-brittle transition commonly observed during laboratory tests.[1] To assure a safer structural design, minimum and maximum reinforcement conditions must be considered, to avoid cracking or crushing failures in the structural elements.[2]

In this context, the application of fracture mechanics concepts to the study of the flexural behavior of reinforced concrete elements leads to important results, as is shown by several studies carried out by Hillerborg et al.,[3] Gustafsson and Hillerborg,[4] Jenq and Shah,[5] Carpinteri,[6-11] Carpinteri et al.,[12] Bosco et al.,[13] Bosco and Carpinteri,[14] and NCHRP,[15] among others.

The effort of adopting effective models that can predict real structural behaviors considering material non-linearities may lead to an optimization of the design process and to a more refined safety assessment for existing structures.

In the present paper, an application of the cohesive/overlapping crack model proposed by Carpinteri et al.[18] is provided, to take into account the effect of a pre-stressing force in a steel strand reinforced concrete cross section. For this purpose, a bond-slip law for pre-stressing reinforcement layers is introduced, and some numerical simulations on prestressed concrete beams are presented, varying both size-scale and reinforcement percentage in the structural elements.

RESEARCH SIGNIFICANCE

In the present work, an investigation on scale effects, mechanical instabilities, and ductile-to-brittle transition in prestressed concrete beams is performed by means of the cohesive/overlapping crack model. The problem of evaluating the rotation capacity of prestressed concrete beams in bending has been little investigated from both the experimental and the analytical point of view during the last decades. Because the development of ductility is influenced by several design parameters, it is difficult to develop a predictive model that can fully describe the mechanical behavior of prestressed concrete. In particular, the role of the size-scale effect, which has been evidenced by some experimental tests, is not yet completely understood. One of the main reasons is the inadequacy of the traditional models based on ad hoc stress-strain constitutive laws. The numerical studies and experimental versus numerical analyses clearly suggest that the model can predict the scale-dependent non-linear behavior of prestressed concrete beams, and that a correct definition of an upper bound[2] represents a strict requirement in the design of this type of structures. As a matter of fact, due to scale effects, the real behavior of prestressed concrete structures may deviate significantly from that predicted by laboratory tests or theory of plasticity and may be highly influenced by crushing failure.

COHESIVE/OVERLAPPING CRACK MODEL

A first description of the cohesive zone was introduced by Dugdale[19] to study the crack-tip plastic zone in metals, and by Barenblatt[20,21] to analyze the cohesive atomic forces in crystals. Then, this concept was extended by Hillerborg et al.[3] and Hillerborg[22] within the fictitious crack model, to study the crack-tip process zone in concrete. Later, the cohesive crack model was adopted by Carpinteri[23] to study the snap-back instabilities in concrete or concrete-like materials, and then by Ruiz et al.[24] to study the non-linear behavior of lightly reinforced concrete beams. This model assumes that, in a beam cross section, the crack starts propagating when the ultimate tensile strength of concrete, σ_t, is reached.[25]

ACI Structural Journal, V. 118, No. 2, March 2021.

MS No. S-2020-065.R1, doi: 10.14359/51728184, received March 20, 2020, and reviewed under Institute publication policies.

In the process zone of a cracked cross section, concrete partially keeps its ability to transfer stresses through the crack faces, and, to model this residual capacity, closing forces depending on the crack width, w^t, are applied.

The stress versus crack opening law can be described as:

$$\sigma = \sigma_t \left(1 - \frac{w^t}{w^t_{cr}}\right) \quad (1)$$

The closing forces resulting from Eq. (1) vanish when the critical value of crack opening, w^t_{cr}, is reached. The area below the σ-w^t curve is the fracture energy of the material, G_F (Fig. 1(b)), and it may be considered as a real material characteristic. Outside the damaged zone, the material still behaves within the elastic field, so that a classical σ-ε constitutive law is adopted (Fig. 1(a)).

Furthermore, the cohesive crack model has been improved also defining an energy brittleness number, s_E, able to interpret the post-peak response of plain concrete structures, showing that their global structural behavior does not depend on single parameters like fracture energy, ultimate tensile strength, or element size, but on their combination.[9,10]

Experimental tests carried out by Kotsovos,[26] van Mier,[27] and Vonk et al.[28] outlined that concrete exhibits strain localization in compression in a similar way to strain softening in tension. Early attempts to describe the compressive non-linear deformation of concrete were proposed by Hillerborg,[29] suggesting a compressive strain localization zone proportional to the compressed depth of the beam, whereas Bažant[30] proposed to set the strain localization length proportional to the characteristic size of the structural element. In both works, the strain localization zone is identified by means of experimental data, and it is not based on theoretical models.

Moreover, a round-robin organized by RILEM TC 148-SSC[31] investigated the effects due to different loading platen typology, shape and size of the specimen, and concrete grade on the strain softening behavior of concrete in compression. The experimental evidence suggested a high correlation between specimen size and post-peak behavior, and, if a displacement is considered in the softening regime rather than the strain, all the curves become almost independent of the specimen size and are restrained within a narrow band. As an example, it is possible to consider the experimental tests carried out by Ferrara and Gobbi[32] at ENEL-CRIS laboratory in Milan. They investigated the structural behavior of three different concrete prisms: 50 x 50 mm (*S*), 100 x 100 mm (*M*), and 150 x 150 mm (*L*), made of three different slenderness ratios (0.5, 1.0, 2.0). In Fig. 2(a) the obtained σ-ε curves are reported. It is possible to observe that specimens have the same elastic ascending branch but once the peak load is reached, a large scattering is registered between them, suggesting that a proper constitutive law for damaged concrete may not be identified in a σ-ε diagram. On the other hand, if a fictitious interpenetration, w^c, is considered, the curves lie within a restrained zone as depicted in Fig. 2(b). The crushing zone can be then represented by a fictitious overlapping, which is mathematically analogous to the fictitious crack opening in tension. It is important to note that from the mathematical point of view, the overlapping

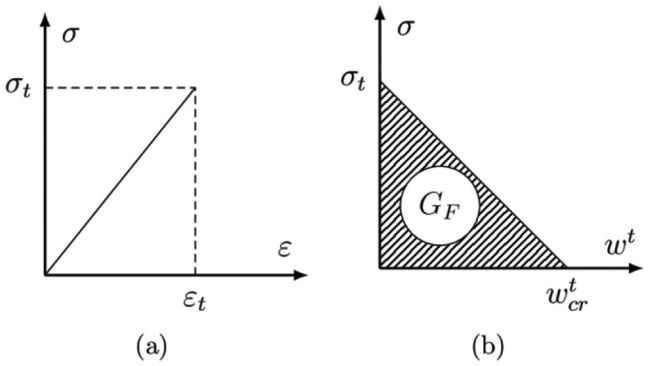

Fig. 1—Cohesive crack model for concrete in tension: (a) linear elastic stress-strain law; and (b) post-peak σ-w^t cohesive relationship.

displacement is a global quantity, and therefore it permits the structural behavior to be characterized without the need for modeling the actual failure mechanism of the specimen into the details, which may vary from pure crushing to diagonal shear failure, to splitting, depending on its size-scale and slenderness. The overlapping crack model,[33] based on a fictitious interpenetration, permits a true material constitutive law to be obtained, independent of the structural size, and it simulates the damage of the material through a virtual overlapping zone in close analogy with the cohesive crack model, offering an effective agreement with experimental results.[31,32] Within this model, a pair of constitutive laws is adopted for concrete in compression: a classical stress-strain law (Fig. 3(a)), valid up to the ultimate compressive strength of concrete, σ_c, and a stress-interpenetration relationship, σ-w^c (Fig. 3), which is effective in the post-peak regime of the structural element subjected to bending. The area subtended by the diagram in Fig. 3(b) represents the crushing energy, G_c, and, in close analogy with the fracture energy, G_F, it can be assumed as a real material constant as experimentally shown by Jansen and Shah.[34]

The crushing energy may be calculated through the Suzuki formula[35]

$$G_c = 80 - 50k_b \quad (2)$$

with $k_b = 40/\sigma_c \leq 1$.

Equation (2) shows that G_c is larger than G_F by two orders of magnitude, due to the better performance of concrete in compression than in tension. As a matter of fact, the critical value of the virtual overlapping, w^c_{cr}, for which the fictitious opening forces vanish, is approximately 10 times w^t_{cr}, as well as the compression strength is one order of magnitude greater than the tensile strength.

For the aim of the present research, a linear σ-w^c law is adopted in the form

$$\sigma = \sigma_c \left(1 - \frac{w^c}{w^c_{cr}}\right) \quad (3)$$

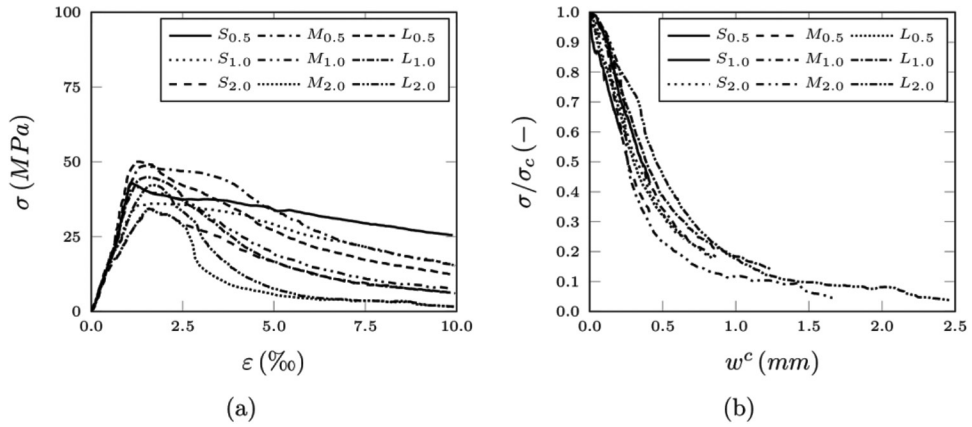

Fig. 2—Uniaxial compression tests[32]: (a) σ-ε relationship; and (b) post-peak σ/σ_c-w^c relationship.

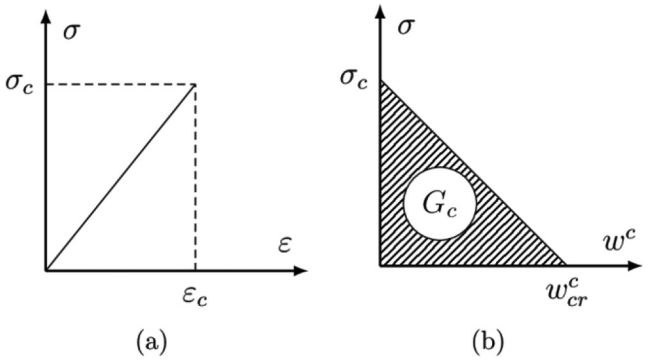

Fig. 3—Overlapping crack model for concrete in compression: (a) linear elastic stress-strain law; and (b) post-peak stress versus fictitious interpenetration relationship.

PRESTRESSING STEEL VERSUS CONCRETE INTERACTION

In the case of a prestressed concrete structural element, because the kinematics of the midspan cross section can be described by means of crack openings and virtual overlappings, a constitutive law that is able to relate crack opening displacements with steel reactions must be adopted. In the present paper, a bond-slip relationship for prestressed reinforcement layer is obtained also considering Model Code 2010.[36] Hence, it is possible to consider a steel strand reinforced concrete element of length L_τ, with a crack as depicted in Fig. 4. Along L_τ, concrete and steel mutually transfer the shearing stresses, $\tau(x)$, which depend on concrete strength, steel surface condition, and slippage developed between the two materials.

The value of L_τ may be found considering the equilibrium equation of the steel strand

$$(\sigma_p - \sigma_0)A_{sp} = \int_0^{L_\tau} \pi\phi\tau(x)dx \tag{4}$$

where $(\sigma_p - \sigma_0)A_{sp}$ represents the increasing force acting in the steel strand due to crack propagation.

On the other hand, it is possible to simplify Eq. (4) considering a mean value of the shearing stresses developed between steel and concrete. Hence, Eq. (4) may be rewritten as

$$L_\tau = \frac{(\sigma_p - \sigma_0)A_{sp}}{\pi\phi\tau_m} \tag{5}$$

where τ_m is a mean value of the shearing stresses along L_τ, which may be fixed in case of indented wire, according to Model Code 2010,[36] as $\tau_m = 1.44\sigma_t$.

The crack opening, from symmetry reasons, may be written as twice the slip between concrete and steel along L_τ. Thus:

$$w^t = 2\int_0^{L_\tau} \left[\varepsilon_s(x) - \varepsilon_{co}(x)\right]dx \tag{6}$$

If a constant shearing stress, τ_m, is admitted between steel and concrete, the increasing force in the steel strand due to cracking varies linearly along L_τ, from a maximum value ($\sigma_p - \sigma_0$) at the cracked section, to 0 at a distance L_τ, as expressed in:

$$\Delta\sigma_s(x) = \left(\sigma_p - \sigma_0\right)\left(1 - \frac{x}{L_\tau}\right) \tag{7}$$

Introducing Eq. (7) into Eq. (6), neglecting the concrete contribution, and considering Eq. (5), it is possible to find:

$$w^t = \frac{(\sigma_p - \sigma_0)^2 A_{sp}}{E_s \pi\phi\tau_m} \tag{8}$$

where σ_p is the steel stress in the cracked cross section; σ_0 is the steel stress at a distance L_τ from the cracked cross section; A_{sp} is the steel area; E_s is the modulus of elasticity of steel; Fig. 2 shows the diameter of the steel strand; and τ_m is the average value of shearing stress exchanged between steel and concrete.

COHESIVE/OVERLAPPING CRACK MODEL FOR PRESTRESSED CONCRETE ELEMENTS

The Cohesive/Overlapping Crack Model[2,16-18,33] can simulate the damage process in the midspan cross section of a prestressed concrete beam by means of a step-by-step numerical approach: the depth of the structural member, b, is divided into (n-1) segments separated by n nodes. To avoid numerical problems, the finite element size has been limited.[37]

Considering the superposition principle, we have (Fig. 5):

$$\{w\} = [K_F]\{F\} + \{K_M\}M + [K_F]\{F_p\} \tag{9}$$

where $\{w\}$ is the vector containing the opening/overlapping displacements; $[K_F]$ is the matrix containing the coefficients of influence for nodal displacements generated by unit forces; $\{K_M\}$ is the vector containing nodal displacements generated by a unit bending moment; M is the value of the bending moment; and $\{F_p\}$ is the vector containing the nodal forces generated by pre-stressing.

Thus, in the general case of Fig. 5, the following conditions are applied:

$$F_i = 0 \text{ for } i = 1,...,(j-1), i \neq r \tag{10a}$$

$$F_i = F_t\left(1 - \frac{w_i}{w_{cr}^t}\right) \text{ for } i = j,...,(m-1) \tag{10b}$$

$$w_i = 0 \text{ for } i = m,...,p \tag{10c}$$

$$F_i = F_c\left(1 - \frac{w_i}{w_{cr}^c}\right) \text{ for } i = (p+1),...,q \tag{10d}$$

$$F_i = 0 \text{ for } i = (q+1),...,n \tag{10e}$$

$$F_i = f(w_i) \text{ for } i = r \tag{10f}$$

where j is the real crack tip; m is the fictitious crack tip; p is the fictitious overlapping zone tip; q is the real overlapping zone tip; and r is the pre-stressing steel node. Equations (9) and (10) constitute a system of $2n$ equations in $(2n+1)$ unknowns. Hence, another condition is needed to calculate the applied external load. The opening and overlapping fictitious crack tips, starting from their initial positions, move forward. At each step, the two external load values that are able to generate the ultimate tensile force, F_t, in node m and the ultimate compresssive force, F_c, in node p are calculated: the actual bending moment, M, is assumed as the minimum load between the two external loads above calculated. Only the tip that reaches the ultimate strength is moved forward: thus, crack opening, and concrete crushing are separated phenomena that take place independently.

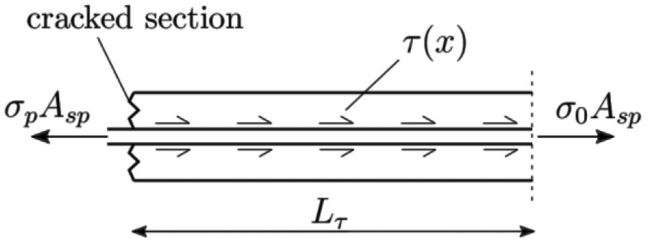

Fig. 4—Prestressing steel versus concrete interaction.

At each step, the rotation angle is computed as:

$$\vartheta = \{D_F\}^T \{F\} + D_M M \tag{11}$$

where $\{D_F\}$ is the vector containing the rotations generated by unit nodal forces; and D_M is the rotation generated by a unit bending moment.

PARAMETRIC ANALYSIS

In Fig. 6 and 7, some case studies of square (t=b) prestressed concrete beams subjected to bending are presented, showing significant scale effects.[38] The prestressing force has been set equal to $1/3 f_y A_{sp}$, where A_{sp} is the steel strand area, and f_y is the steel yield strength equal to 1640 MPa. The reinforcement has been positioned to keep the ratio between the beam effective depth and the beam depth as d/b = 0.9. The concrete tensile strength, σ_t, is assumed equal to 4 MPa, whereas the compressive strength, σ_c, is equal to 40 MPa. The critical value of crack opening is w^t_{cr} = 0.04 mm, whereas the critical value for concrete virtual overlapping is w^c_{cr} = 1.5 mm. The concrete stress-strain laws, both for tension and compression, have been assumed according to Eq. (1) and (3). The reinforcement ratio, ρ_p, varies between 0.1% and 1.0%, whereas the beam depth, b, varies between 400 and 1500 mm.

In the case of low steel percentages (Fig. 6), it is possible to observe a first elastic branch up to the complete exploitation of the pre-stressing force, when the concrete fracturing takes place. After this first peak load, a snap-back due to cracking appears,[39,40] and a second ascending branch due to an increase in the steel reaction is revealed. Hence, the steel reinforcement reaches its yielding, and a horizontal plateau is described. The width of this horizontal plastic branch is inversely proportional to the beam depth, b, and

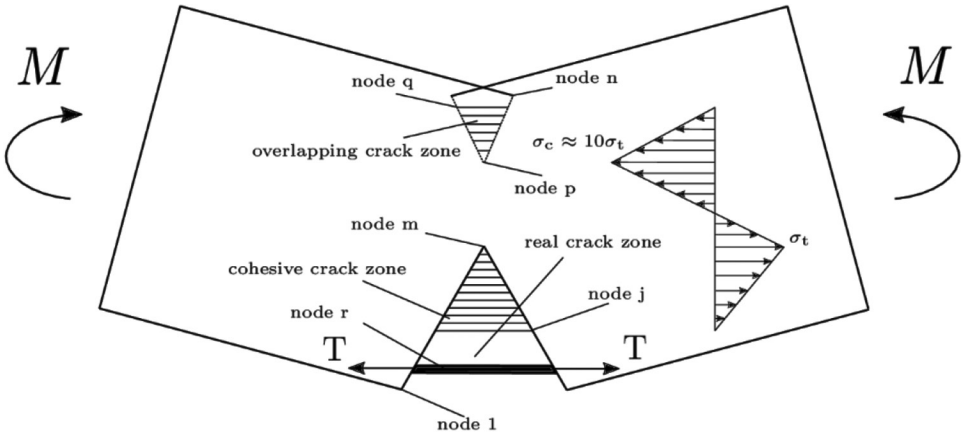

Fig. 5—Cohesive/overlapping crack model.

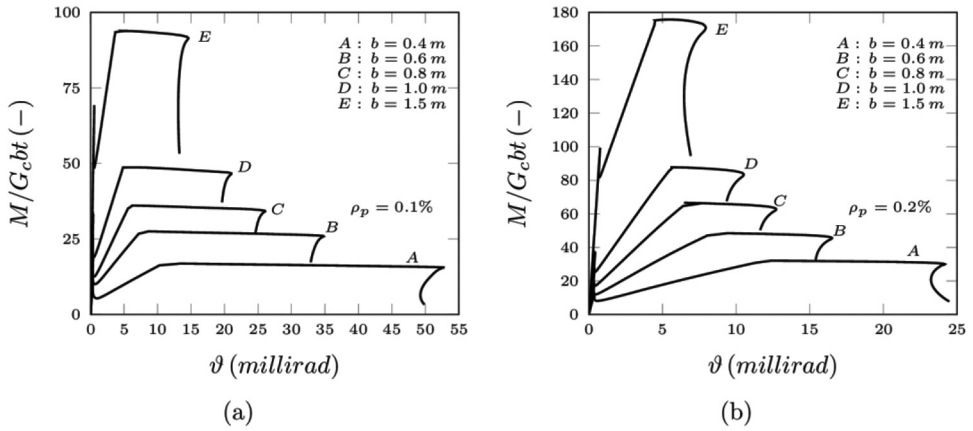

Fig. 6—Non-dimensional load versus rotation curves for: (a) ρ_p = 0.1%; and (b) ρ_p = 0.2%.

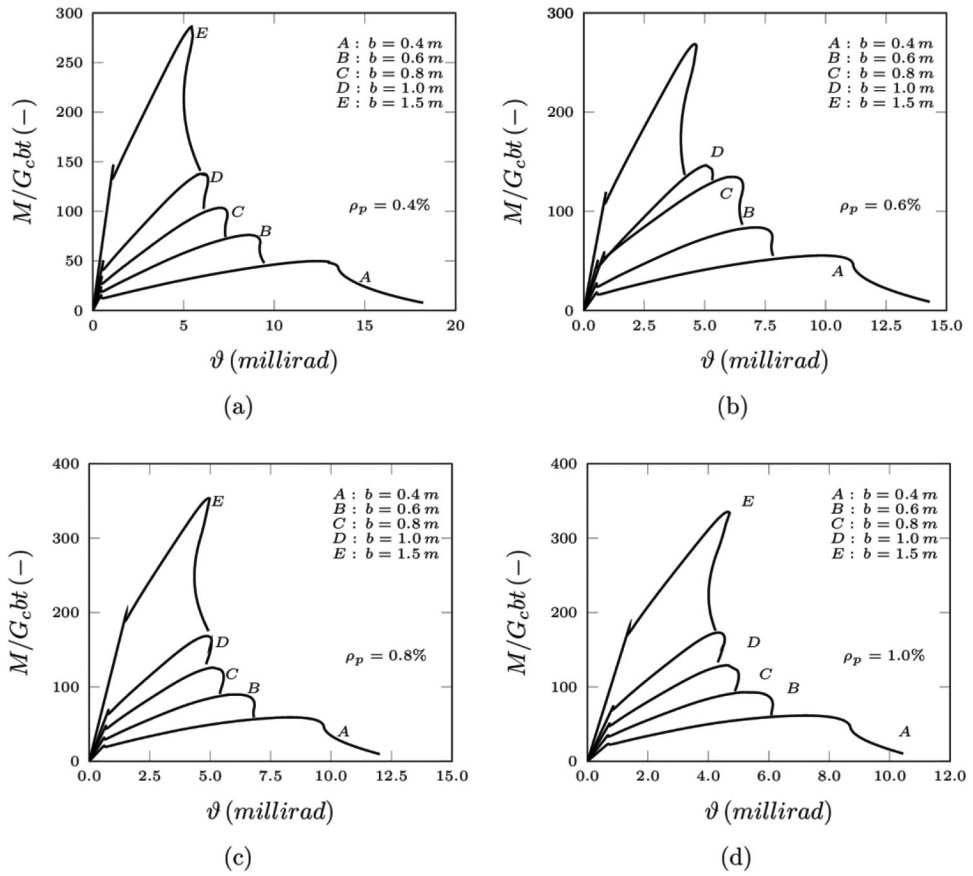

Fig. 7—Non-dimensional load versus rotation curves for: (a) ρ_p = 0.4%; (b) ρ_p = 0.6%; (c) ρ_p = 0.8%; and (d) ρ_p = 1.0%.

reinforcement percentage, ρ_p.[17] Eventually, a snap-back is determined, due to the unstable concrete crushing brittle behavior.

For reinforcement percentages larger than 0.4% (Fig. 7), it is possible to observe a substantial disappearance of steel yielding, and a major role played by concrete crushing on the global behavior of the structural element subjected to bending. This is mainly due to the larger value of the force exerted by the pre-stressing steel reinforcement. In these last cases characterized by larger reinforcement percentage, ρ_p, the limit established by a maximum reinforcement condition appears to be strict.

NUMERICAL VERSUS EXPERIMENTAL INVESTIGATION

In the following, a numerical versus experimental comparison is proposed for the mechanical behavior of prestressed concrete beams subjected to bending. To perform this comparison, the wide experimental campaign carried out by Warwaruk et al.[41] is discussed.

This experimental campaign was conducted on 82 simply supported prestressed concrete beams considering several bonding conditions. The tests results show three typical stages in the load-deflection curves: the first stage is linear elastic, and it is characterized by the mechanical properties of the undamaged cross section of the beam. The second phase, after the first cracking load, is characterized by a cracked cross

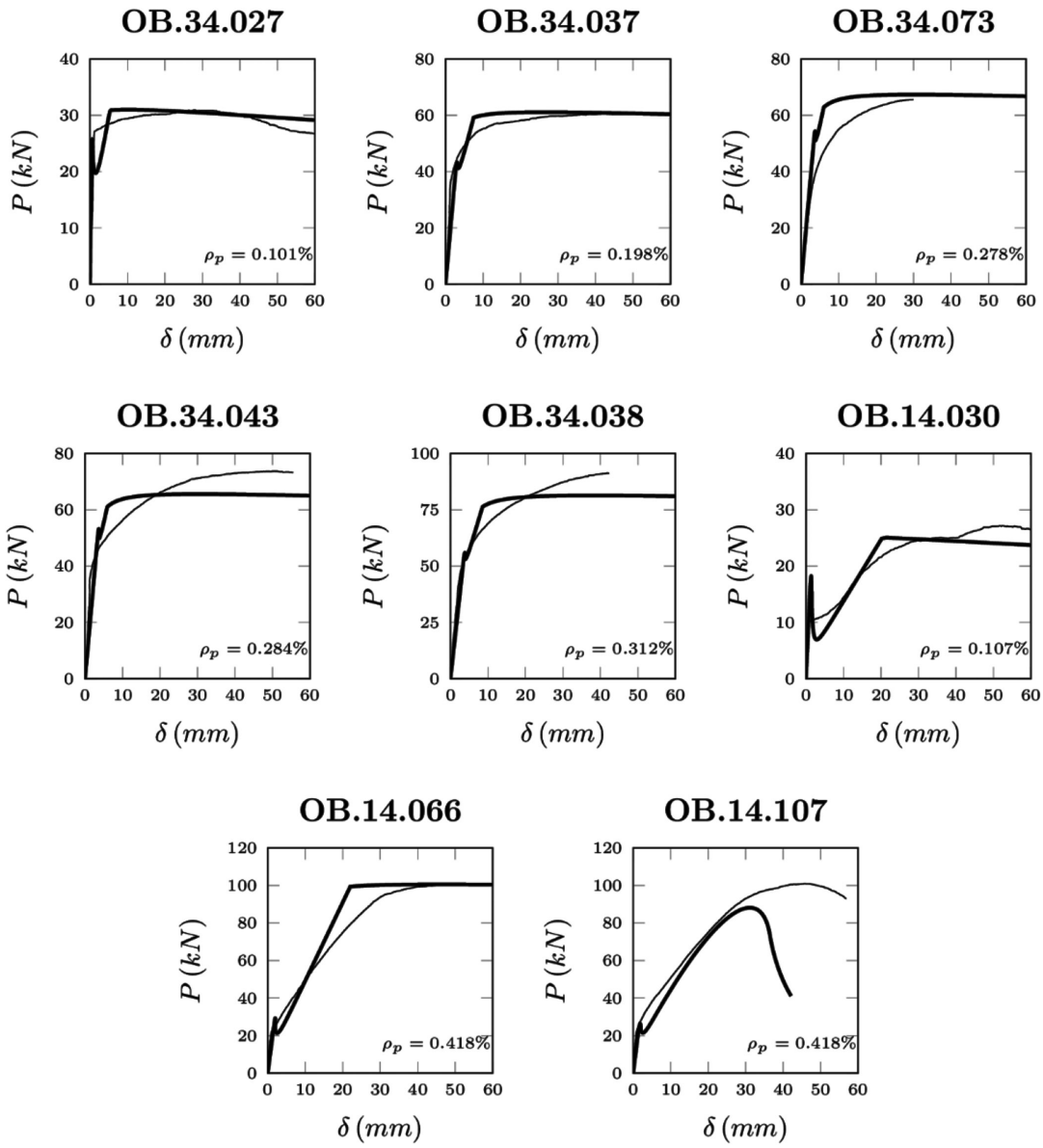

Fig. 8—Numerical (thick) versus experimental (thin) curves for prestressed concrete specimens with reinforcement percentage, ρ_p, lower than or equal to 0.4%.

section with the steel reinforcement acting within the elastic field. The third phase is characterized by a change in the curve slope, due to the plasticity of the steel reinforcement. On the other hand, the whole experimental campaign shows that these three phases are present only for prestressed concrete beams having low reinforcement ratios. In beams having higher reinforcement ratios, the third phase is absent, because the steel is not able to reach yielding, and a substantial disappearance of the beam plastic rotational capacity arises, as predicted by the cohesive/overlapping crack model.

In the following, experimental versus numerical curves representing the structural behavior of the specimens subjected to four-point bending tests and having a cross section of 152.4 x 304.8 mm are reported. Mechanical parameters, reinforcement ratio, and pre-stressing force for each tested beam are reported in Table 1. The tensile strength of concrete, σ_t, and fracture energy, G_F are determined according to Model Code 2010[36]

$$\sigma_t = 0.3\sigma_c^{2/3} \tag{12}$$

$$\sigma_t = 2.12\ln[1+0.1(\sigma_c+8)] \tag{13}$$

$$G_F = 73/1000(\sigma_c+8)^{0.18} \tag{14}$$

Equation (12) is valid for concrete having $\sigma_c \leq 50$ MPa, whereas Eq. (13) is valid for concrete having $\sigma_c > 50$ MPa. The crushing energy, G_c, is determined according to Eq. (2).

In Fig. 8, the experimental tests (thin curves) performed on prestressed concrete beams with reinforcement percentage lower than 0.4% provide a structural behavior that can be accurately described by the cohesive/overlapping crack model (thick curves): from the first mechanical instabilities (snap-back and/or snap-through) following the complete exploitation of the pre-stressing force, through the activation of the steel reinforcement, up to its yielding, when a plastic plateau is observed. It is worth noting the different behaviors between OB.14.066 and OB.14.107 detected by means

Table 1—Mechanical parameters of the tested beams[41]

Beam	d (mm)	ρ_p (%)	f_y (MPa)	σ_0 (MPa)	σ_c (MPa)	σ_t (MPa)	G_F (N/mm)	G_c (N/mm)	w^t_{cr} (mm)	w^c_{cr} (mm)
OB.34.027	244	0.101	1564.03	826.80	27.38	2.73	0.139	30.000	0.102	2.191
OB.34.037	242	0.198	1564.03	804.75	33.52	3.12	0.143	30.000	0.092	1.790
OB.34.073	235	0.278	1260.87	817.15	51.41	4.11	0.152	41.100	0.074	1.599
OB.34.043	230	0.284	1260.87	813.02	48.69	4.00	0.151	38.924	0.075	1.599
OB.34.038	231	0.312	1536.47	826.80	44.62	3.77	0.149	35.178	0.079	1.577
OB.14.030	229	0.107	1543.36	130.91	23.72	2.48	0.136	30.000	0.110	2.529
OB.14.066	234	0.418	1543.36	131.60	41.79	3.61	0.148	32.145	0.082	1.538
OB.14.107	237	0.418	1543.36	140.56	25.66	2.61	0.137	30.000	0.105	2.339
OB.14.175	207	0.656	1543.36	146.07	27.79	2.75	0.139	30.000	0.101	2.159
OB.14.157	237	0.870	1543.36	140.56	38.93	3.45	0.146	30.000	0.085	1.541
OB.14.244	203	0.916	1543.36	139.18	28.14	2.78	0.139	30.000	0.100	2.132
OB.34.290	203	0.953	1260.87	777.88	23.28	2.45	0.136	30.000	0.111	2.578

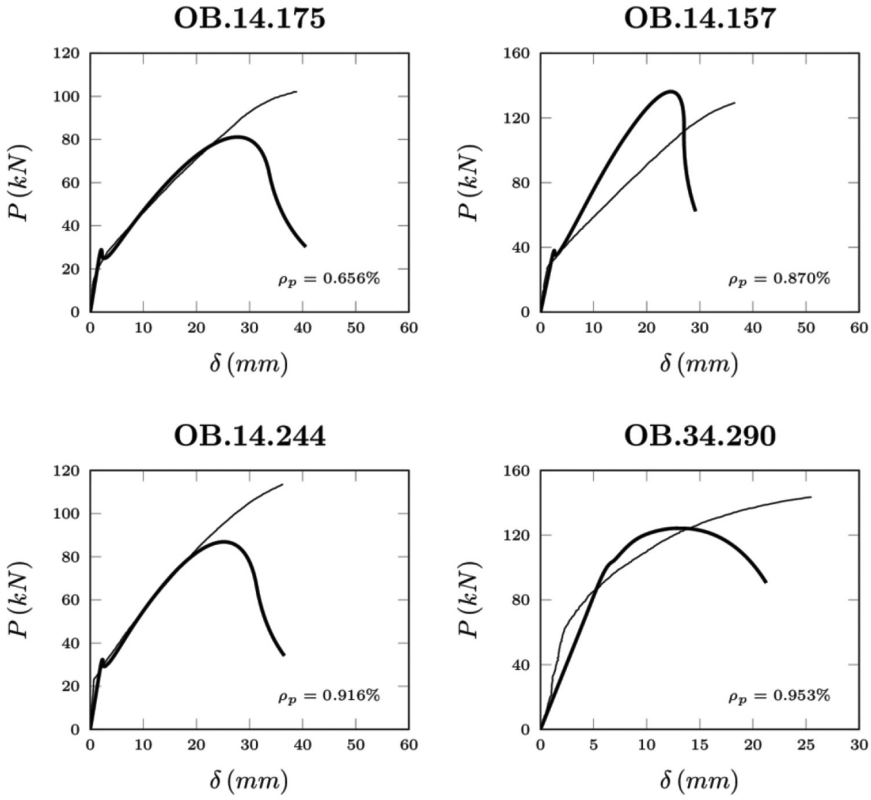

Fig. 9—Numerical (thick) versus experimental (thin) curves for prestressed concrete specimens with reinforcement percentage, ρ_p, larger than 0.4%.

of the cohesive/overlapping crack model. These specimens have the same reinforcement ratio and pre-stressing force, but a different concrete compressive strength, σ_c, generating an ultimate behavior characterized by steel yielding in OB.14.066, and by concrete crushing in OB.14.107, due to its lower σ_c. An enhanced compressive behavior is experimentally observed for specimen OB.14.107, recognizing a stirrups confinement effect in the midspan region of the tested beam, which is able to delay the concrete crushing failure.

In Fig. 9, the specimens with reinforcement percentage larger than 0.4% are analyzed, showing a structural behavior more unsafe than that obtained in the case of low steel percentages, because the rotational capacity of the prestressed beams is considerably reduced, and also concrete crushing could precede steel yielding, as predicted by the cohesive/overlapping crack model. Hence, in the post-peak regime, the beams could exhibit an ultimate snap-back in the load carrying capacity due to an unstable growth of the concrete crushing zone, usually hidden by the displacement control of the test (abrupt interruption). It is worth noting that the concrete beams with reinforcement percentage lower than 0.4% (Fig. 8) provide a rotational capacity up to 60 mm, whereas the specimens with reinforcement percentage larger

than 0.4% (Fig. 9) show a significant increase in brittleness with a rotational capacity reduced to 30 mm.

The analyses discussed earlier demonstrate the capability of the cohesive/overlapping crack model in predicting the non-linearities developed by prestressed concrete beams under loading, showing catastrophic snap-back branches after concrete cracking or crushing. These mechanical instabilities are hidden in the experimental curves, because the tests were carried out using the loading control until the first cracking load appears (snap-through), and using the displacement control in the post-peak regime (final abrupt interruption). These control parameters do not allow the detection of local or global snap-back branches, because they are not a monotonically increasing function of time, such as the crack length.[42]

CONCLUSIONS

The application of fracture mechanics concepts[43-47] to the study of prestressed concrete structural behavior can provide a correct estimation of the scale effects on the maximum reinforcement percentage, which requires a thorough knowledge of the complex non-linear phenomena characterizing the concrete crushing failure. If one simply considers a traditional stress-strain curve for concrete which includes softening, they may not capture the catastrophic post-peak behavior characterizing cracking and crushing failures, (that is, the snap-back instability). Thus, to fully describe the concrete cracking process, the cohesive crack model must be adopted, whereas to describe the concrete crushing, the overlapping crack model must be employed. In this way, by means of the cohesive/overlapping crack model it is possible to address the lack of knowledge about the field in which prestressed concrete structures can develop a safe ductile behavior, formulating new standard requirements for an effective structural design.

In the present work, an investigation on scale effects, mechanical instabilities, and ductile-to-brittle transition in prestressed concrete beams is performed by means of a non-linear fracture mechanics model. The cohesive/overlapping crack model is able to predict both cracking and crushing failures in prestressed concrete elements, and the transition between these two failure mechanisms increasing the beam size and/or the reinforcement percentage. Due to its analytic nature, this model allows to perform large-scale assessments, leading to a refinement of the standards included in the international codes of practice. On the other hand, such complex analyses may also be performed by means of the finite element method with a great deal of effort, because strain softening materials exhibit spurious mesh sensitivity, low convergence rate, and results that are highly dependent on mesh refinement.[48,49]

Finally, the present analysis points out the importance of the maximum reinforcement ratio, to guarantee a minimum rotational capacity for safety reasons and seismic energy dissipation, avoiding the rise of concrete crushing without steel yielding. For low reinforcement percentages, steel yielding precedes concrete crushing, and large plateau are described in the load versus displacement diagrams. However, because the width of the plastic plateau decreases as size or reinforcement ratio increase, until it disappears for large structural sizes and/or high steel percentages, a maximum reinforcement condition may be identified as the largest reinforcement percentage for which steel yielding precedes concrete crushing.

AUTHOR BIOS

Federico Accornero *is Postdoctoral Fellow at Politecnico di Torino, Turin, Italy. He received his PhD in structural engineering with distinction from Politecnico di Torino in 2014. His research interests include fracture mechanics, concrete structures, masonry arch bridges, and acoustic emission monitoring.*

Renato Cafarelli *is a PhD Student at Politecnico di Torino. His research interests include fracture mechanics and concrete structures.*

Alberto Carpinteri *is Chair of Structural Mechanics at Politecnico di Torino, is presently the Head of the engineering division in the European Academy of Sciences.*

NOTATION

A_{sp}	=	pre-stressing steel area
b	=	beam depth
$\{D_F\}$	=	vector of rotations generated by unit forces
D_M	=	rotation generated by unit moment
d	=	beam effective depth
E_s	=	modulus of elasticity of steel
$\{F\}$	=	vector of nodal forces
$\{F_p\}$	=	vector of nodal forces generated by pre-stressing
f_y	=	steel yield strength
G_c	=	crushing energy
G_F	=	fracture energy
$[K_F]$	=	matrix of nodal displacements generated by unit forces
$\{K_M\}$	=	vector of nodal displacements generated by unit bending moment
L_τ	=	transferring length of shear stresses between steel and concrete
M	=	bending moment
n	=	number of nodes
t	=	beam thickness
$\{w\}$	=	vector of nodal displacements
w^c	=	fictitious interpenetration
$w^c{}_{cr}$	=	critical value of fictitious interpenetration (overlapping law)
w^t	=	crack opening
$w^t{}_{cr}$	=	critical value of crack opening (cohesive law)
ε_c	=	ultimate compressive strain of concrete
ε_{co}	=	strain in concrete
ε_s	=	strain in steel
ε_t	=	ultimate tensile strain of concrete
ϕ	=	steel strand diameter
ρ_p	=	pre-stressing steel reinforcement ratio
σ	=	stress
σ_c	=	compressive strength of concrete
σ_p	=	pre-stressing steel stress (in cracked section)
σ_t	=	tensile strength of concrete
σ_0	=	pre-stressing stress (imposed by jacks)
τ	=	steel/concrete interfacial shear stress
τ_m	=	mean value of the steel/concrete interfacial shear stress
ϑ	=	rotation

REFERENCES

1. Carpinteri, A.; Marega, C.; and Savadori, A., "Ductile-Brittle Transition by Varying Structural Size," *Engineering Fracture Mechanics*, V. 21, No. 2, 1985, pp. 263-271. doi: 10.1016/0013-7944(85)90015-3

2. Carpinteri, A., and Corrado, M., "Upper and Lower Bounds for Structural Design of RC Members with Ductile Response," *Engineering Structures*, V. 33, No. 12, 2011, pp. 3432-3441. doi: 10.1016/j.engstruct.2011.07.007

3. Hillerborg, A.; Modéer, M.; and Petersson, P.-E., "Analysis of Crack Formation and Crack Growth in Concrete by Means of Fracture Mechanics and Finite Elements," *Cement and Concrete Research*, V. 6, No. 6, 1976, pp. 773-781. doi: 10.1016/0008-8846(76)90007-7

4. Gustafsson, P. J., and Hillerborg, A., "Sensitivity in Shear Strength of Longitudinally Reinforced Concrete Beams to Fracture Energy of Concrete," *ACI Structural Journal*, V. 85, No. 3, May-June 1988, pp. 286-294.

5. Jenq, Y. S., and Shah, S. P., "Shear Resistance of Reinforced Concrete Beams – A Fracture Mechanics Approach," *Fracture Mechanics: Application to Concrete*, SP-118, American Concrete Institute, Farmington Hills, MI, 1990, pp. 237-258.

6. Carpinteri, A., "A Fracture Mechanics Model for Reinforced Concrete Collapse," *IABSE Reports of the Working Commissions*, 1981.

7. Carpinteri, A., "Sensitivity and Stability of Progressive Cracking in Plain and Reinforced Cement Composites," *International Journal of Cement Composites and Lightweight Concrete*, V. 4, No. 1, 1982, pp. 47-56. doi: 10.1016/0262-5075(82)90007-0

8. Carpinteri, A., "Stability of Fracturing Process In RC Beams," *Journal of Structural Engineering*, ASCE, V. 110, No. 3, 1984, pp. 544-558. doi: 10.1061/(ASCE)0733-9445(1984)110:3(544)

9. Carpinteri, A., "Interpretation of the Griffith Instability as a Bifurcation of the Global Equilibrium," *Application of Fracture Mechanics to Cementitious Composite (edited by Surenda P. Shah), NATO ASI Series, Series E: Applied Sciences,* V. 94, 1985, pp. 287-316.

10. Carpinteri, A., "Size Effects on Strength, Toughness, and Ductility," *Journal of Engineering Mechanics*, ASCE, V. 115, No. 7, 1989, pp. 1375-1392. doi: 10.1061/(ASCE)0733-9399(1989)115:7(1375)

11. Carpinteri, A., *Minimum Reinforcement in Concrete Members*, Elsevier, 1999.

12. Carpinteri, A.; Colombo, G.; and Giuseppetti, G., "Accuracy of the Numerical Description of the Cohesive Crack Propagation," *Fracture Toughness and Fracture Energy of Concrete,* Elsevier Science Publisher, 1985, pp. 189-195.

13. Bosco, C.; Carpinteri, A.; and Debernardi, P. G., "Fracture of Reinforced Concrete: Scale Effects and Snap-Back Instability," *Engineering Fracture Mechanics*, V. 35, No. 4-5, 1990, pp. 665-677. doi: 10.1016/0013-7944(90)90149-B

14. Bosco, C., and Carpinteri, A., "Softening and Snap-through behavior of Reinforced Elements," *Journal of Engineering Mechanics*, ASCE, V. 118, No. 8, 1992, pp. 1564-1577. doi: 10.1061/(ASCE)0733-9399(1992)118:8(1564)

15. NCHRP, "LRFD Minimum Flexural Reinforcement Requirements," *National Cooperative Highway Research Program (NCHRP) Research Report 906*, 2019.

16. Carpinteri, A.; Corrado, M.; Paggi, M.; and Mancini, G., "Cohesive Versus Overlapping Crack Model for a Size Effect Analysis of RC Elements in Bending," *Proceedings of the 6th International Conference on Fracture Mechanics of Concrete and Concrete Structures*, V. 2, 2007, pp. 655-663.

17. Carpinteri, A.; Corrado, M.; Mancini, G.; and Paggi, M., "Size-Scale Effects on Plastic Rotational Capacity of Reinforced Concrete Beams, *ACI Structural Journal*, V. 106, No. 6, Nov.-Dec. 2009, pp. 887-896.

18. Carpinteri, A.; Corrado, M.; and Paggi, M., "An Integrated Cohesive/Overlapping Crack Model for the Analysis of Flexural Cracking and Crushing in RC Beams," *International Journal of Fracture*, V. 161, No. 2, 2010, pp. 161-173. doi: 10.1007/s10704-010-9450-4

19. Dugdale, D. S., "Yielding of Steel Sheets Containing Slits," *Journal of the Mechanics and Physics of Solids*, V. 8, No. 2, 1960, pp. 100-104. doi: 10.1016/0022-5096(60)90013-2

20. Barenblatt, G. I., "The Formation of Equilibrium Cracks during Brittle Fracture, General Ideas and Hypothesis, Axially Symmetric Cracks," *Journal of Applied Mathematics and Mechanics*, V. 23, 1959, pp. 434-444.

21. Barenblatt, G. I., "The Mathematical Theory of Equilibrium Cracks in Brittle Fracture," *Advances in Applied Mechanics*, V. 7, 1962, pp. 55-129. doi: 10.1016/S0065-2156(08)70121-2

22. Hillerborg, A., "Numerical Methods to Simulate Softening and Fracture of Concrete," *Fracture Mechanics of Concrete: Structural Application and Numerical Calculation (edited by George C. Sih and Angelo Di Tommaso)*, 1985, pp. 141-170.

23. Carpinteri, A., "Cusp Catastrophe Interpretation of Fracture Instability," *Journal of the Mechanics and Physics of Solids*, V. 37, No. 5, 1989, pp. 567-582. doi: 10.1016/0022-5096(89)90029-X

24. Ruiz, G.; Elices, M.; and Planas, J., "Size Effect and Bond-Slip Dependence of Lightly Reinforced Concrete Beams," *Minimum Reinforcement in Concrete Members* (edited by Alberto Carpinteri), 1999, pp. 67-97.

25. Petersson, P.-E., "Crack Growth and Development of Fracture Zone in Plain Concrete and Similar Materials," PhD thesis, 1981, Lund University.

26. Kotsovos, M. D., "Effect of Testing Techniques on the Post-Ultimate Behaviour of Concrete in Compression," *Matériaux et Construction*, V. 16, 1983, pp. 3-12.

27. van Mier, J. G. M., "Strain-Softening of Concrete under Multiaxial Loading Conditions," PhD thesis, 1984, Eindhoven University of Technology, Eindhoven, the Netherlands.

28. Vonk, R. A.; Rutten, H. S.; Van Mier, J. G. M.; and Fijneman, H. J., "Influence of Boundary Conditions on Softening of Concrete Loaded in Compression," *Fracture of Concrete and Rock – Recent Developments (edited by S.P. Shah, S.E. Swartz and B. Barr)*, Elsevier Applied Science, 1989, pp. 711-720

29. Hillerborg, A., "Fracture Mechanics Concepts Applied to Moment Capacity and Rotational Capacity of Reinforced Concrete Beams," *Engineering Fracture Mechanics*, V. 35, No. 1-3, 1990, pp. 233-240. doi: 10.1016/0013-7944(90)90201-Q

30. Bažant, Z. P., "Identification of Strain-Softening Constitutive Relation from Uniaxial Tests by Series Coupling Model for Localization," *Cement and Concrete Research*, V. 19, No. 6, 1989, pp. 973-977. doi: 10.1016/0008-8846(89)90111-7

31. van Mier, J. G. M.; Shah, S. P.; Arnaud, M.; Balayssac, J. P.; Bascoul, A.; Choi, S.; Dasenbrock, D.; Ferrara, G.; French, C.; Gobbi, M. E.; Karihaloo, B. L.; König, G.; Kotsovos, M. D.; Labuz, J.; Lange-Kornbak, D.; Markeset, G.; Pavlovic, M. N.; Simsch, G.; Thienel, K.-C.; Turatsinze, A.; Ulmer, M.; van Geel, H. J. G. M.; van Vliet, M. R. A.; and Zissopoulos, D., "Strain-softening of Concrete in Uniaxial Compression," *Materials and Structures*, V. 30, No. 4, 1997, pp. 195-209. doi: 10.1007/BF02486177

32. Ferrara, G., and Gobbi, M.E., "Strain Softening of Concrete under Compression," *Report to RILEM Committee 148*, 1995.

33. Carpinteri, A.; Corrado, M.; Mancini, G.; and Paggi, M., "The Overlapping Crack Model for Uniaxial and Eccentric Concrete Compression Tests," *Magazine of Concrete Research*, V. 61, No. 9, 2009, pp. 745-757. doi: 10.1680/macr.2008.61.9.745

34. Jansen, D. C., and Shah, S. P., "Effect of Length on Compressive Strain Softening of Concrete," *Journal of Engineering Mechanics*, ASCE, V. 123, No. 1, 1997, 25 pp., doi: 10.1061/(ASCE)0733-9399(1997)123:1(25)

35. Suzuki, M.; Akiyama, M.; Matsuzaki, H.; and Dang, T. H., "Concentric Loading Test of RC Columns with Normal and High-Strength Materials and Averaged Stress-Strain Model for Confined Concrete Considering Compressive Fracture Energy," *Proceedings of the 2nd Fib Congress*, 2006

36. International Federation for Structural Concrete, *fib Model Code for Concrete Structures*, International Federation for Structural Concrete, Ernst&Sohn, 2013.

37. Carpinteri, A., and Colombo, G., "Numerical Analysis of Catastrophic Softening Behavior (Snap-Back Instability)," *Computers & Structures*, V. 31, No. 4, 1989, pp. 607-636. doi: 10.1016/0045-7949(89)90337-4

38. Carpinteri, A., and Accornero, F., "Rotation Versus Curvature Fractal Scaling in Bending Failure," *Physical Mesomechanics*, V. 22, No. 1, 2019, pp. 46-51. doi: 10.1134/S1029959919010089

39. Carpinteri, A., and Accornero, F., "Multiple Snap-Back Instabilities in Progressive Microcracking Coalescence," *Engineering Fracture Mechanics*, V. 187, 2018, pp. 272-281. doi: 10.1016/j.engfracmech.2017.11.034

40. Carpinteri, A., and Accornero, F., "The Bridged Crack Model with Multiple Fibers: Local Instabilities, Scale Effects, Plastic Shake-Down, and Hysteresis," *Theoretical and Applied Fracture Mechanics*, V. 104, 2019, 102351 pp., doi: 10.1016/j.tafmec.2019.102351

41. Warwaruk, J.; Sozen, M. A.; and Siess, C. P., *Investigation of Prestressed Reinforced Concrete for Highway Bridges, Part III*, 1962, University of Illinois.

42. Biolzi, L.; Cangiano, S.; Tognon, G.; and Carpinteri, A., "Snap-Back Softening Instability in High Strength Concrete Beams," *Materials and Structures*, V. 22, No. 6, 1989, pp. 429-436. doi: 10.1007/BF02472220

43. Wittmann, F. H., "Fracture Mechanics of Concrete," *Elsevier*, 1983.

44. Elfgren, L., ed., "Fracture Mechanics of Concrete Structures: From Theory to Applications," Report of the Technical Committee 90 – FMA Fracture Mechanics to Concrete/Applications, RILEM (the International Union of Testing and Research Laboratories for Materials and Structures), Chapman and Hall, Taylor and Francis Group, 1989

45. Elfgren, L., and Shah, S. P., eds., "Analysis of Concrete Structures by Fracture Mechanics: Proceedings of a RILEM Workshop dedicated to Professor Arne Hillerborg," Chapman and Hall, Taylor and Francis Group, 1991.

46. Shah, S. P., and Carpinteri, A., "Fracture Mechanics Test Methods for Concrete," Report of the Technical Committee 89 FMT Fracture Mechanics of Concrete – Test Methods, Chapman and Hall, 1991.

47. Bažant, Z. P., and Planas, J., *Fracture and Size Effect in Concrete and Other Quasibrittle Materials*, CRC Press, Boca Raton, FL, 1997

48. ACI Committee 446, "Fracture Mechanics of Concrete: Concepts, Models and Determination of Materials Properties (ACI 446.1R-91)," American Concrete Institute, Farmington Hills, MI, 1999, 146 pp.

49. ACI Committee 446, "Finite Element Analysis of Fracture in Concrete Structures (ACI 446.3R-97)," American Concrete Institute, Farmington Hills, MI, 1997, pp. 33.